THE ACCELERATED WEATHERING OF A RADIOACTIVE LOW-ACTIVITY WASTE GLASS UNDER HYDRAULICALLY UNSATURATED CONDITIONS: EXPERIMENTAL RESULTS FROM A PRESSURIZED UNSATURATED FLOW TEST

RADIOACTIVE WASTE MANAGEMENT AND DISPOSAL

KEYWORDS: *immobilized low-activity waste glass, pressurized unsaturated flow system, accelerated weathering*

E. M. PIERCE,* B. P. McGRAIL, M. M. VALENTA, and D. M. STRACHAN
Pacific Northwest National Laboratory, Environmental Technology Directorate
P.O. Box 999, MS: K6-81, Richland, Washington 99352

Received November 18, 2005
Accepted for Publication January 30, 2006

To predict the long-term fate of low- and high-level waste forms in the subsurface over geologic timescales, it is important to understand how the formation of an alteration phase or phases will affect radionuclide release from the corroding waste forms under repository-relevant conditions. To generate data to conduct performance assessment calculations for the low-activity waste (LAW) integrated disposal facility at the Hanford Site in southeastern Washington state, accelerated weathering experiments are being conducted with the pressurized unsaturated flow (PUF) test method to evaluate the long-term release of radionuclides from immobilized LAW (ILAW) glasses. The radionuclide release rate is a key parameter affecting the overall performance of the LAW disposal facility.

Currently, there are three other accelerated weathering test methods being used to evaluate the long-term durability of glasses: product consistency test, vapor hydration test, and unsaturated drip test. In contrast to these test methods, PUF tests mimic the hydraulically unsaturated open-flow and transport conditions expected in the near-field vadose zone environment, allow the corroding waste form to achieve its final reaction state, and accelerate the hydrolysis and aging processes by as much as 50 times over conventional static tests run at the same temperature.

In this paper, we discuss the results of an accelerated weathering experiment conducted with the PUF apparatus to evaluate the corrosion rate of an ILAW glass, LAWAN102, made with actual Hanford waste taken from Tank 241-AN-102 (U). Results from this PUF test with LAWAN102 glass showed that after 1.5 yr of testing, the corrosion rate, based on B release, reached a steady-state release of 0.010 ± 0.003 $g\,m^{-2}\,day^{-1}$, which is approximately eight times lower than other glasses previously tested. These results indicate that ^{99}Tc is being released from the glass congruently, whereas U is being controlled by the formation of a solubility-limiting phase or phases. These results also highlight the importance of being able to predict, with some level of certainty, the alteration phase or phases that will form and how the formation of these phases may impact the release, retention, and transport of radionuclides from the glass under the hydraulically unsaturated open flow and transport conditions that are expected in the LAW integrated disposal facility.

I. INTRODUCTION

The facilities located on the Hanford Site in southeastern Washington state have been used extensively by the United States to produce nuclear materials for the U.S. strategic defense arsenal. Currently, the Hanford Site is under the stewardship of the U.S. Department of Energy (DOE). A large inventory of radioactive and mixed waste, resulting from the production of nuclear materials, has accumulated in 177 underground single- and

*E-mail: Eric.Pierce@pnl.gov

double-shell tanks located in the central plateau of the Hanford Site in southeastern Washington state.[1] The DOE is proceeding with plans to permanently dispose of the liquid and solid wastes contained in the tanks. Wastes will first be retrieved from the tanks, the sludges (insoluble material) washed, and the liquids processed to generate a high-level waste (HLW) fraction and a low-activity waste (LAW) fraction. The HLW fraction will contain the bulk of the radionuclides, in particular the actinides. The low-activity fraction will contain predominately inactive sodium from the sodium salts and ^{99}Tc as the major radionuclide. Both waste streams will be converted to glass for disposal with the high-level fraction destined for the proposed geologic repository at Yucca Mountain and the low-activity fraction destined to stay on the Hanford Site in the Integrated Disposal Facility[2] (IDF).

In the work reported here, we have been testing glasses that are a part of the LAW disposal effort. To formulate the immobilized low-activity waste (ILAW) glasses, a waste retrieval schedule has been developed at Bechtel Hanford Company, a Hanford contractor for the DOE. The formulation for ILAW glasses was originally divided into three classifications or compositional envelopes: envelopes A, B, and C (Ref. 3). The current waste retrieval schedule results in waste batches that will be used to formulate batches of glass at the waste treatment plant (WTP) as an alternative to the compositional envelope production process. Each glass batch produced by the WTP must have certain properties that fit within a processing and performance envelope.[4]

Before the ILAW can be placed into a near surface of the disposal system on the Hanford Site (i.e., IDF), the DOE must approve a performance assessment, which is a document that describes the long-term impact of the disposal facility on public health and environmental resources.[5] A critical component of the performance assessment will be to provide quantitative estimates of radionuclide release rates from the engineered portion of the disposal facility (source term). These data will be used for reactive transport modeling simulations of the IDF for ILAW using the Subsurface Transport Over Reactive Multiphases (STORM) code.[6] A key parameter in providing quantitative estimates of radionuclide release is information on the long-term corrosion rate of the glass waste form under repository-relevant conditions. To obtain this information requires an extensive set of laboratory tests that are used to evaluate different aspects of the glass-water interaction, as described in a strategic plan by McGrail et al.[5,7,8] For a detailed discussion of the overall testing strategy used for the IDF performance assessment, consult McGrail et al.[5,7,8]

The pressurized unsaturated flow (PUF) test method is one of the laboratory test methods used to evaluate the long-term durability of ILAW glasses. This method has several advantages over other accelerated test methods including the unsaturated drip test[9] (UDT), the vapor hydration test[10] (VHT), and the product consistency test[11,12] (PCT), which are briefly discussed below. The PUF test method provides information on the (a) alteration phase or phases that form as a result of accelerated weathering; (b) evolution in the solution chemistry that occurs as a result of the glass-water interaction, which allows for model validation and direct determination of the corrosion rate; and (c) glass-water reaction under hydraulically unsaturated conditions similar to those expected in a disposal-system environment. The information obtained from conducting PUF tests is a critical component for quantifying the long-term durability of and radionuclide release from glass or any other waste form after disposal. The pros and cons of the other test methods being used are discussed next.

The long-term corrosion of nuclear waste glass, HLW and LAW glass, has been studied for more than two decades.[10,12–22] Although these results are useful, the test methods used limit their applicability for model validation. The majority of the available results on the accelerated weathering of these waste forms have been produced with static test methods, such as the UDT (Ref. 9), VHT (Ref. 10), and PCT (Refs. 11 and 12).

As part of the UDT, water is allowed to drip intermittently onto a glass sample and collect in the bottom of a vessel. This test provides a large amount of information on the alteration phase or phases that form as well as any changes in solution chemistry that occur as a result of glass-water interaction. Although critical information is obtained, little is known about the solution-to-volume ratio (S/V), which is likely to vary during the test. Results from Ebert and Bates[17] have shown that during the early stages of testing changes to the S/V will have a profound effect on the reaction path taken during the glass-water reaction. These changes in the S/V represent an unconstrained variable that makes data interpretation difficult.

The VHT is another unsaturated test method. A specimen is suspended in a container with a specified volume of water required to obtain the target water vapor saturation in the test vessel. Similar to the UDT, this test method provides critical information on the secondary-phase paragenesis, but it also has significant drawbacks. First, the glass corrosion rate cannot be directly measured, because no information is obtained on the solution chemistry. Therefore, the rate is subjectively measured by determining the alteration layer thickness or the amount of unreacted glass remaining.[23] Second, the amount of condensed liquid on the sample is not directly quantifiable, probably changes over time, and may depend on physical or chemical properties of the test material.

Contrary to the VHT and the UDT, the PCT is a water-saturated static test. The reaction products are allowed to accumulate in the aqueous phase, thus altering the solution chemistry in contact with the glass. Although information on the solution chemistry is obtained, the changes to the solution chemistry measured in

this closed-system test may not be representative of the solution chemistry that is expected in an open-system repository. For example, PUF test results with LD6-5412 and LAWA33 glasses suggest that in the PUF test the aging processes are accelerated by as much as 50 times in comparison to the PCT method run at the same temperature.[24] This observed acceleration in the aging process is probably the result of the differences in the glass-water reaction rate, the solution chemistry, and the rate of alteration phase formation in the PUF test in comparison to the PCT.

More important, the closed-system test conditions under which the UDT, the VHT, and the PCT are conducted are quite different from the open system expected in a subsurface burial facility, such as the IDF. In contrast to the PUF, these test methods do not allow for mass transport processes to occur, such as the transport of water and atmospheric gases. The integration of dynamic flow and transport processes, as well as allowing the corroding glass (or another waste form) to achieve its final reaction state, makes the PUF test method an ideal method for evaluating the long-term corrosion of glass under conditions more relevant to a repository. Although the PUF system has been used in accelerated weathering tests on several waste forms, the focus of this discussion will be on results obtained from a 1.5-yr accelerated weathering experiment on an LAW glass, LAWAN102, made with actual Hanford waste taken from Tank 241-AN-102 (U).

TABLE I

Normalized Composition (Mass %) of the Unreacted LAWAN102 Glass and LAWC22 Glass

Oxide	LAWAN102	LAWC22
Al_2O_3	6.19	6.08
B_2O_3	10.05	10.06
CaO	6.24	5.12
Cl	0.03	0.09
Cr_2O_3	0.08	0.02
Fe_2O_3	6.94	5.43
HfO_2	0.05	ND[a]
K_2O	0.19	0.10
Li_2O	2.76	2.51
MgO	1.41	1.51
MnO	0.03	0.04
MoO_3	0.003	ND[a]
Na_2O	11.23	14.40
NiO	0.08	0.03
P_2O_5	0.17	0.17
PbO_2	0.02	0.02
Re_2O_7	ND[a]	0.01
Rh_2O_3	0.001	ND[a]
SO_3	0.31	0.34
SiO_2	47.41	46.67
SnO_2	0.002	ND[a]
SrO	0.02	ND[a]
TcO_2	0.0001	ND[a]
TiO_2	1.24	1.14
UO_2	0.001	ND[a]
V_2O_5	0.02	ND[a]
ZnO	2.99	3.07
ZrO_2	2.54	3.03

[a]ND = not detected.

II. EXPERIMENTAL MATERIALS AND METHODS

II.A. Material Preparation

Glass LAWAN102 was prepared by mixing ~16 ℓ of the pretreated low-activity fraction of the supernate, from Hanford Tank 241-AN-102 (U), with measured amounts of dried reagent-grade glass-forming chemicals in a 600-mL platinum-gold crucible.[25] All glass-forming chemicals were specified by Vitreous State Laboratory (VSL) and were based on the composition of VSL LAWC21 glass.[3] The pretreatment process removes ^{90}Sr and transuranics (TRUs) from the supernate by Sr-TRU precipitation[26] and the majority of the ^{137}Cs and ^{99}Tc by ion exchange from the supernate.[27] For additional details on the fabrication of LAWAN102 glass, consult Crawford et al.[25] and the references contained therein. The final composition of LAWAN102 glass is given in Table I along with a similar glass, LAWC22. Glass LAWC22 is a prototypic ILAW glass that was made with nonradioactive simulants and based on a glass formulation to treat LAW from Tank-241-AN-107 (Ref. 3).

Samples of LAWAN102 glass were crushed in a ceramic ball mill and sieved into the desired size fraction, 250 to 170 μm, with American Society for Testing and Materials standard sieves.[28] After being sized, each sample was washed in deionized water (DIW), sonicated in DIW, and rinsed in ethanol to remove any fine-grain adherence. After being rinsed with ethanol, the sample was dried in a 90°C oven. Scanning electron microscope (SEM) and transmission electron microscope (TEM) images of the unreacted glass are provided in Fig. 1 and suggest that although the glass is homogenous and not phase separated, microscopic Si-rich inclusions, probably quartz, are visible under a TEM at a 7.5×10^4 times magnification. This was confirmed with X-ray diffraction (XRD) analysis of the unreacted LAWAN102 glass.

The specific surface area of each sample was calculated with a geometric formula, Eq. (1) from McGrail et al.,[29]

$$S = \frac{3m}{\rho r} \quad , \tag{1}$$

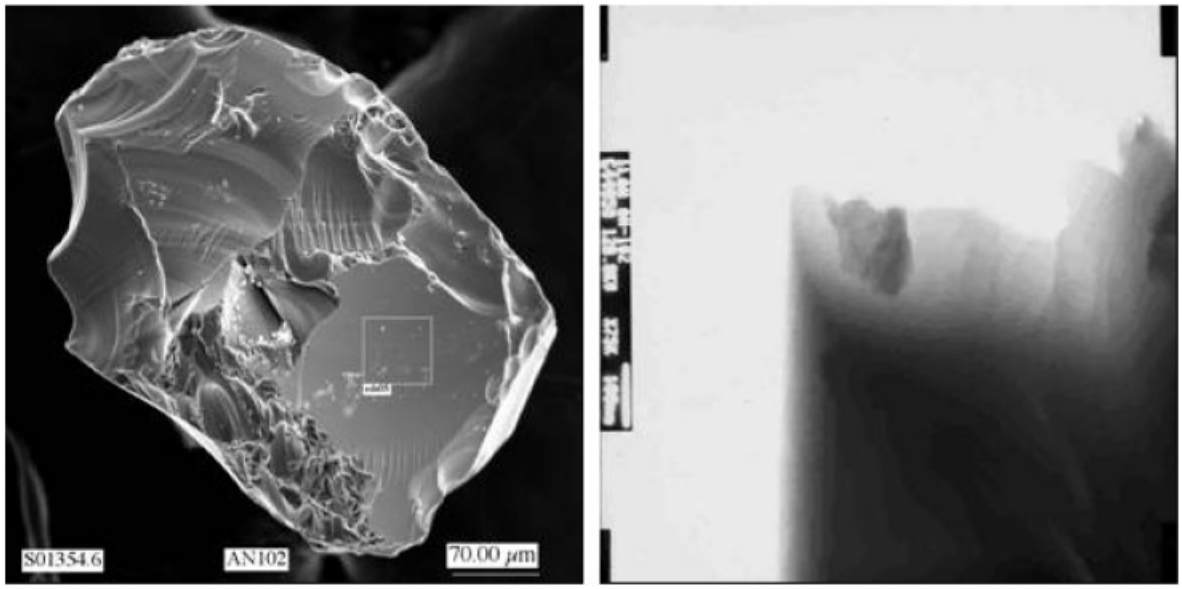

Fig. 1. Scanning (right) and transmission (left) electron micrographs of an unreacted particle of LAWAN102. Although not visible in SEM analysis, TEM analysis of the unreacted glass at 7.5×10^4 times magnification illustrated a small Si-enriched inclusion, probably quartz, shown in the upper left corner of the image. Images taken from McGrail et al.[36]

where

S = surface area (m^2)

m = mass of glass (g)

ρ = glass density ($g\,m^{-3}$) ($\rho = 2.667 \times 10^6\ g\,m^{-3}$ measured with a Micromeritics He-gas pycnometer)

r = average radius (m).

This formula assumes that the particles are spherical; that the size of the grains are normally distributed; and that surface pits, cracks, and other forms of surface roughness do not affect the surface area. Although all three of these assumptions may not be valid, the results from experiments with LAW glass monoliths[30] and natural glass samples[31] suggest the geometric surface area best represents the overall glass surface area. Therefore, all the reported rates in this study are normalized to the geometric surface area.

II.B. PUF Test Method

The PUF apparatus allows for accelerated weathering experiments to be conducted under hydraulically unsaturated conditions, thereby mimicking the open-flow and transport properties of the disposal system environment while allowing the corroding glass to achieve a final reaction state. The PUF apparatus provides the capability to vary the volumetric water content from saturation to 20% or less, minimize the flow rate to increase liquid residence time, and operate at a maximum temperature of 99°C. The PUF column operates under a hydraulically unsaturated condition by creating a steady-state vertical water flow, while maintaining uniform water content throughout the column; by using gravity to assist in drainage; and by maintaining a constant pressure throughout the column. Constant pressure is maintained with a porous Ti plate and gas pressure.

This system and test procedure have been described previously by McGrail et al.,[32–34] and only a general description will be provided here. The PUF system has a 7.62-cm-long and 1.91-cm-diam column fabricated from a chemically inert material, polyetheretherketone, so that dissolution reactions are not influenced by interaction with the column material (Fig. 2). A porous Ti plate with a nominal pore size of 0.2 μm is sealed in the bottom of the column to ensure an adequate pressure differential for the conductance of fluid while operating under unsaturated conditions.[35] Titanium is chosen because it is highly resistant to corrosion and has excellent wetting properties. Once the porous Ti plate is water saturated, water but not air is allowed to flow through the 0.2-μm pores, as long as the applied pressure differential does not exceed the air entry relief pressure, referred to as the bubble pressure, of the Ti plate. If the pressure differential is exceeded, air will escape through the plate and compromise the ability to maintain unsaturated flow conditions in the column. The computer control system runs LabVIEW (National Instruments Corporation) software for logging test data from several thermocouples, pressure sensors, inline sensors for effluent pH and

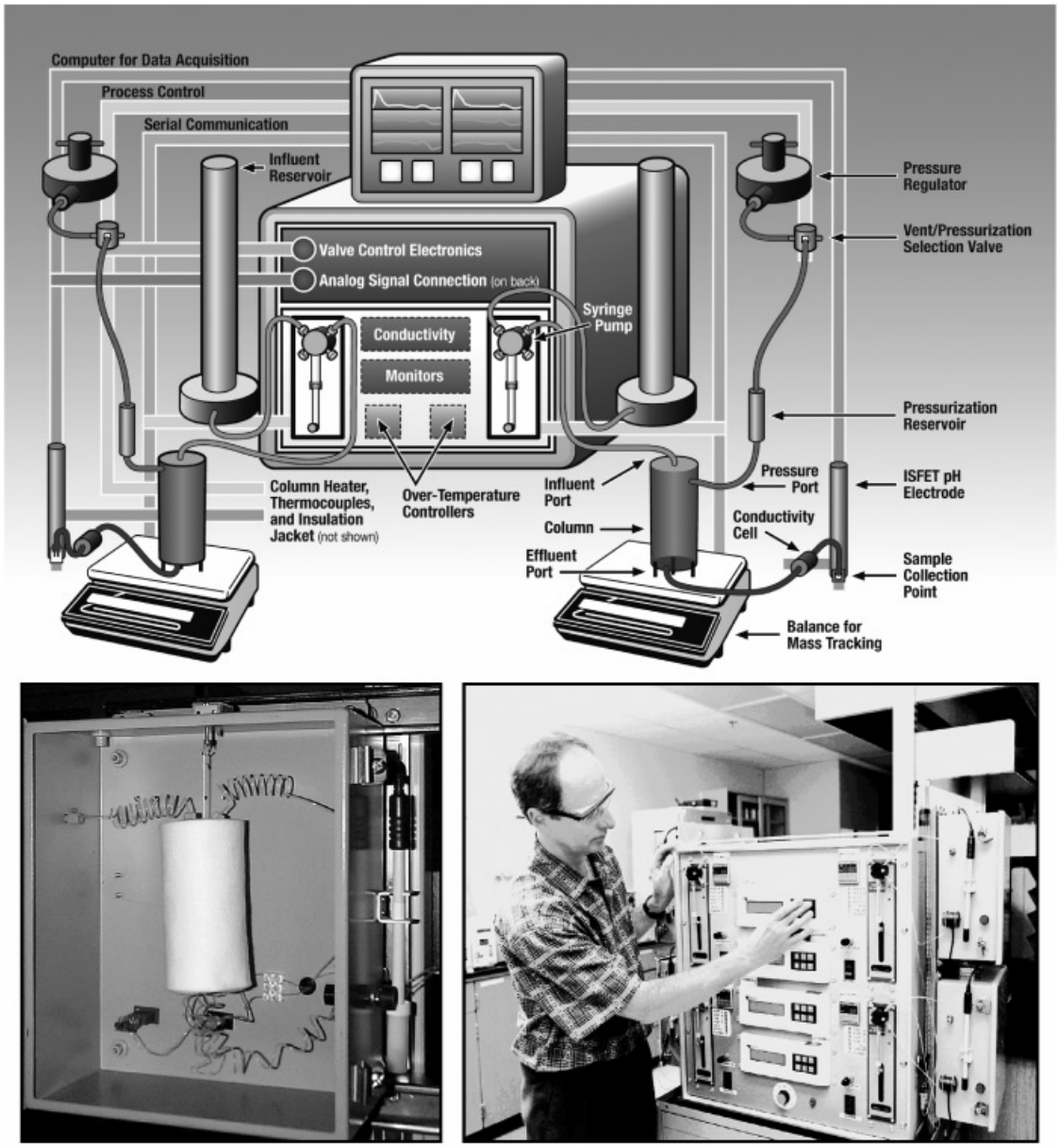

Fig. 2. Top: schematic of the second-generation PUF apparatus, which has the ability to conduct two simultaneous tests. Bottom left: the third-generation PUF apparatus, which has the ability to conduct four simultaneous tests. Bottom right: the PUF box (gray box), insulation wrapped column (center of the box), strain gauge (center of the box above the column), pressure/PUF port Teflon line (top left of the column), influent solution Teflon line (top right of the column), effluent solution Teflon line (bottom of the column), thermocouples [type J (blue connector) and type T (black connector) shown inside the box with black/red wire], pH probe (outside the box shown in white), and collection vial (outside the box connected to the pH probe). The third-generation PUF apparatus was used to conduct the LAWAN102 experiment discussed in this paper.

conductivity, and from an electronic strain gauge that measures column mass to accurately track water mass balance and saturation level. The column also includes a PUF port, which is an electronically actuated valve that periodically vents the column gases. The purpose of column venting is to prevent reduction in the partial pressure of important gases, especially O_2 and CO_2, which may be consumed in a variety of chemical reactions.

The PUF column was packed with 33.55 g of crushed and cleaned LAWAN102 glass, which resulted in a fill volume of 12.58 cm^3 and a void volume of 9.14 cm^3. The mass difference between the packed and the empty

columns was used to calculate the initial porosity of ~0.42 ± 0.03 (unitless). After packing, the column was vacuum saturated with DIW at ambient temperature. A temperature controller was then programmed to heat the column to 90°C in ~1 h (1°C min^{-1}). The column initially was allowed to desaturate by gravity drainage during heating and was also vented periodically to maintain an internal pressure less than the bubble pressure of the porous plate. After reaching 90°C, the influent valve was opened, and influent was set to a flow rate of 2 mL day^{-1}. The influent reservoir containing DIW was maintained at ambient temperature and periodically refilled during the test. Column venting was set to occur once an hour, so the partial pressure of O_2 and CO_2 could remain relatively constant. Effluent samples were collected into tared vials from which samples were extracted and acidified for elemental analysis with inductively coupled plasma (ICP)–optical emission spectroscopy and ICP-mass spectrometry.

After 560 days (~1.5 yr), the PUF experiment was terminated. Upon termination, the reacted solids were subsampled as found (loose and moist particles) and as a function of depth (3- to 5-mm intervals). The subsamples were placed in glass vials, dried at room temperature in a sealed container with $CaSO_4$ desiccant, and analyzed for reaction products with XRD and SEM.

Powder XRD patterns were recorded in a Scintag automated powder diffractometer (Model 3520) with Cu K_α radiation. The results were analyzed with the computer program JADE (Materials Data Inc., in Livermore, California) combined with the Joint Committee on Powder Diffraction Standards' International Center for Diffraction Data (Newtown Square, Pennsylvania) database.

A JEOL JSM-840 SEM was used to determine particle morphology and size. The microscope is equipped with an Oxford Links ISIS 300 energy dispersive X-ray analysis system (EDS) that was used for qualitative elemental analysis. Operating conditions were 20 keV for SEM imaging and 100 live seconds with 20 to 30% dead time for the EDS analyses. The EDS analyses of particles are limited to elements with atomic weights heavier than boron. Photomicrographs of high-resolution secondary electron images were obtained as digital images and stored in electronic format. The SEM-EDS mounts consisted of double-sided carbon tape attached to a standard aluminum planchet. The sample mounts were place in a vacuum sputter and carbon coated to improve the conductivity of the samples and thus the quality of the SEM images and EDS signals.

II.C. PUF Dissolution Rate and Experimental Error

The results of chemical analyses on collected effluent samples are used to calculate a normalized release rate according to McGrail et al.[36]:

$$r_i = \frac{4\varepsilon q(c_{i,L} - c_{i,b})}{\theta S(1-\varepsilon)\rho\pi d^2 L f_i} \quad , \tag{2}$$

where

r_i = normalized dissolution (release) rate of the i'th element (g m^{-2} day^{-1})

$c_{i,L}$ = effluent concentration of the i'th element (g m^{-3})

$c_{i,b}$ = background concentration of the i'th element (g m^{-3})

d = column diameter (m)

L = column length (m)

q = volumetric flow rate (m^3 day^{-1})

S = specific surface area of the glass sample (m^2 g^{-1})

ε = porosity (unitless)

ρ = glass density (g m^{-3})

f_i = mass fraction of the i'th element (unitless)

θ = volumetric water content (unitless).

The volumetric water content is calculated based on the mass of a volume of water in a fixed column volume, accounting for changes in the solution density resulting from temperature changes. The background concentration for most elements is typically below the estimated quantification limit (EQL) for the respective analysis. The EQL is defined as the lowest calibration standard that can be determined reproducibly during an analytical run within 10% of the certified value multiplied by the sample dilution factor. In cases where the analyte is below the EQL, the background concentration of the element is set at the value of the EQL.

The normalized release rate for an element is based on the solution concentration divided by the mass fraction f_i of the element in the waste form. Boron is considered the most reliable indicator of matrix dissolution and congruent release, because it serves as a glass network former, like Si and Al, and is not sequestered by alteration phases after being released from the glass.[37] Unlike B, other elements may be retained in alteration phases during the glass-water reaction. Therefore, an element with a lower normalized release rate, in comparison to B, indicates the element is being retained by an alteration phase or phases, whereas a higher normalized release rate suggests preferential release, such as alkali-hydrogen ion exchange.

An estimate of the experimental uncertainty associated with the normalized dissolution rate is calculated from standard error propagation theory, assuming the variables in Eq. (2) are uncorrelated. For uncorrelated random errors, the standard deviation of a function $f(x_1, x_2, \ldots, x_n)$ is given by

$$\sigma_f = \sqrt{\sum_{i=1}^{n} \left(\frac{\partial f}{\partial x_i} \right)^2 \sigma_i^2} \ , \tag{3}$$

where

σ_f = standard deviation of the function f

x_i = parameter i

σ_i = standard deviation of parameter i.

Assuming that the error associated with the background concentration ($c_{i,b}$), diameter (d), and column length (L) are negligible compared with the other variables, the relative standard deviation is given by

$$\sigma_{r_i} = r_i \sqrt{\left(\frac{\tilde{\sigma}_\varepsilon}{1-\varepsilon} \right)^2 + \left(\frac{\tilde{\sigma}_{c_{i,L}}}{1 - c_{i,b}/c_{i,L}} \right)^2 + \tilde{\sigma}_Q^2 + \tilde{\sigma}_\theta^2 + \tilde{\sigma}_S^2 + \tilde{\sigma}_\rho^2 + \tilde{\sigma}_{f_i}^2} \ , \tag{4}$$

where the tilde over the σ symbol signifies the relative standard deviation for the subscripted parameter. In calculating the error bounds with Eq. (4), typical fixed relative standard deviations have been estimated based upon the repeatability of laboratory measurements:

$$\tilde{\sigma}_\varepsilon = 6\% \ , \quad \tilde{\sigma}_S = 20\% \ , \quad \tilde{\sigma}_Q = 2\%$$

$$\tilde{\sigma}_\rho = 5\% \ , \quad \tilde{\sigma}_{c_{i,L}} = 10\% \ , \quad \tilde{\sigma}_{f_i} = 10\% \ .$$

The value of $\tilde{\sigma}_\theta$ is calculated from the variation in water content recorded by the data acquisition system over the discrete interval between each fluid sampling. A Microsoft Excel macro is available to perform this calculation directly in the spreadsheet used to store the sensor data.

III. RESULTS

III.A. Computer-Monitored Test Metrics

Results from the computer-monitored test metrics are shown in Fig. 3. The sensor data were smoothed with a bisquare weighting method where the smoothed datum

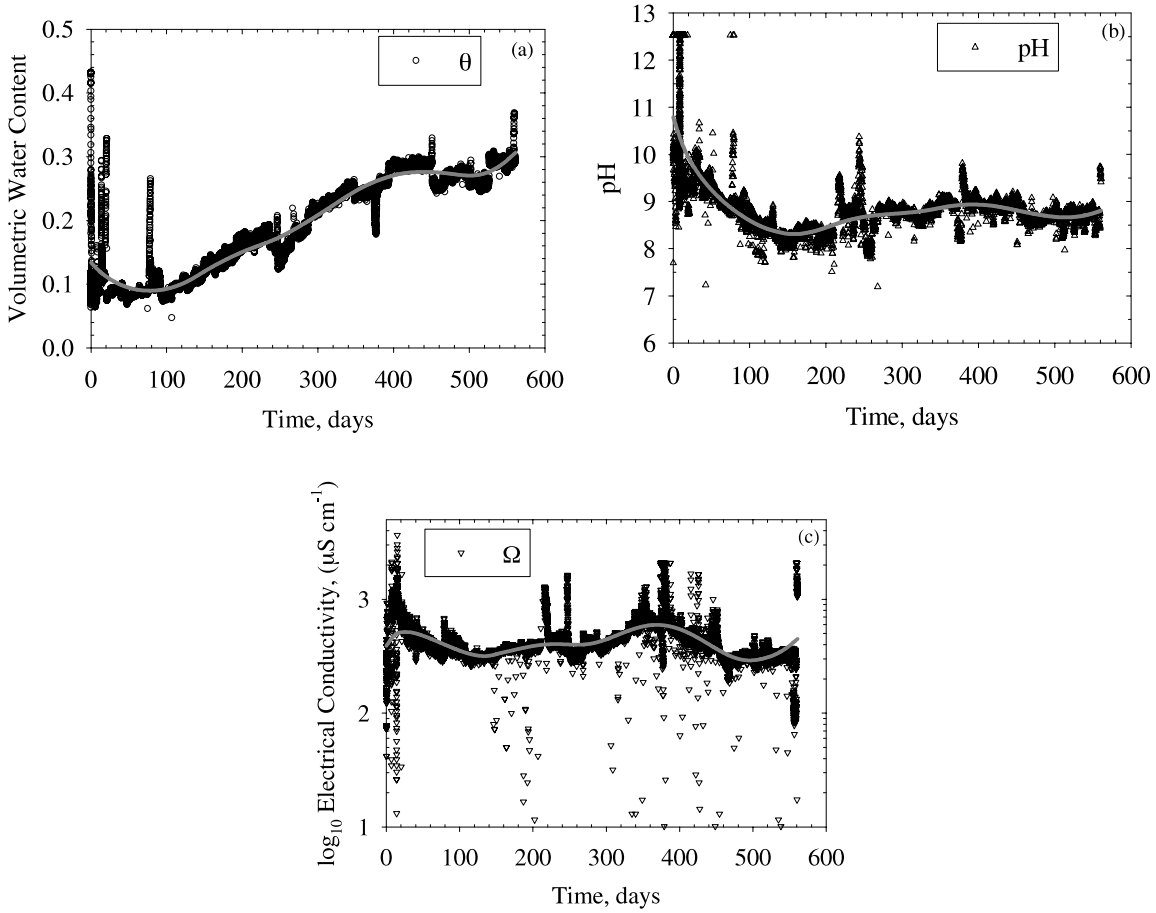

Fig. 3. Computer-monitored test metrics—(a) volumetric water content, (b) pH, and (c) electrical conductivity—from PUF tests with LAWAN102 glass. The gray lines are bisquare smoothed fits to the raw data and are provided as a guide to the eye.

y_s is given by $y_s = (1 - \omega^2)^2$. The parameter ω is a weighting coefficient calculated from a window surrounding the smoothing location in the set of the independent variables. A low-order polynomial regression (order 2 in this case) is used to compute ω for each smoothed value. The smoothed data are provided as lines and were used to make qualitative assessments of the results (Fig. 3). Figure 3a illustrates that volumetric water content (θ) was steady between 0 and 100 days, increased between day 100 and 400, and reached a plateau after 450 days of testing until the experiment was terminated. The increase in the volumetric water content between day 100 and 400 is because of changes in the hydraulic properties of the glass powder in the column caused by an increase in reaction products as well as an increase in the waters of hydration associated with the alteration phases. The formation of finely grained alteration phases on the surface of the glass causes the retention of water in the column to increase and the rate of water flow out of the column to gradually decrease; this results in a gradual increase in the water content as seen in Fig. 3a. This trend has also been observed in the early stages of a PUF test with a less durable glass, LD6-5412 (Ref. 34), as well as with other long-term PUF tests conducted with other glasses and waste forms.[24,33,38,39] McGrail et al.[34] measured the hydraulic conductivity as a function of PUF test duration using the centrifugation method (i.e., unsaturated flow apparatus[40,41]). The results from McGrail et al.[34] illustrated that changes in the water-retention characteristics of the hydrated glass are manifested as an increase in the volumetric water content during the PUF test and are related to the initial precipitation of zeolitic alteration phases, phillipsite ($KCaAl_3Si_5O_{16}$) and gobbinisite ($Na_4CaAl_6Si_{10}O_{32}\cdot 12H_2O$).

Unlike the volumetric water content, the pH and electrical conductivity (Ω) remained relatively constant (Figs. 3b and 3c). These results suggest a moderate corrosion rate, evident from the moderate pH and electrical conductivity. Results contained in Figs. 3b and 3c also suggest that steady state was achieved between the 50th and 100th day of testing; this was also observed in the solution chemistry results.

III.B. Solution Chemistry

Results from the analyses of effluent samples are provided in Fig. 4. The release of elements from the column illustrates a general trend of decreasing concentration with increasing reaction time. The normalized concentrations of B, K, Li, Na, S, and ^{99}Tc are as much as 1×10^3 times greater than Al, Ca, and U, but only 10 to 20 times greater than Si (Fig. 4). The normalized concentration (NC_i) was calculated from the element concentrations in the effluent solutions with Eq. (5)

$$NC_i = \frac{(c_{i,L} - c_{i,b})}{f_i} \quad , \tag{5}$$

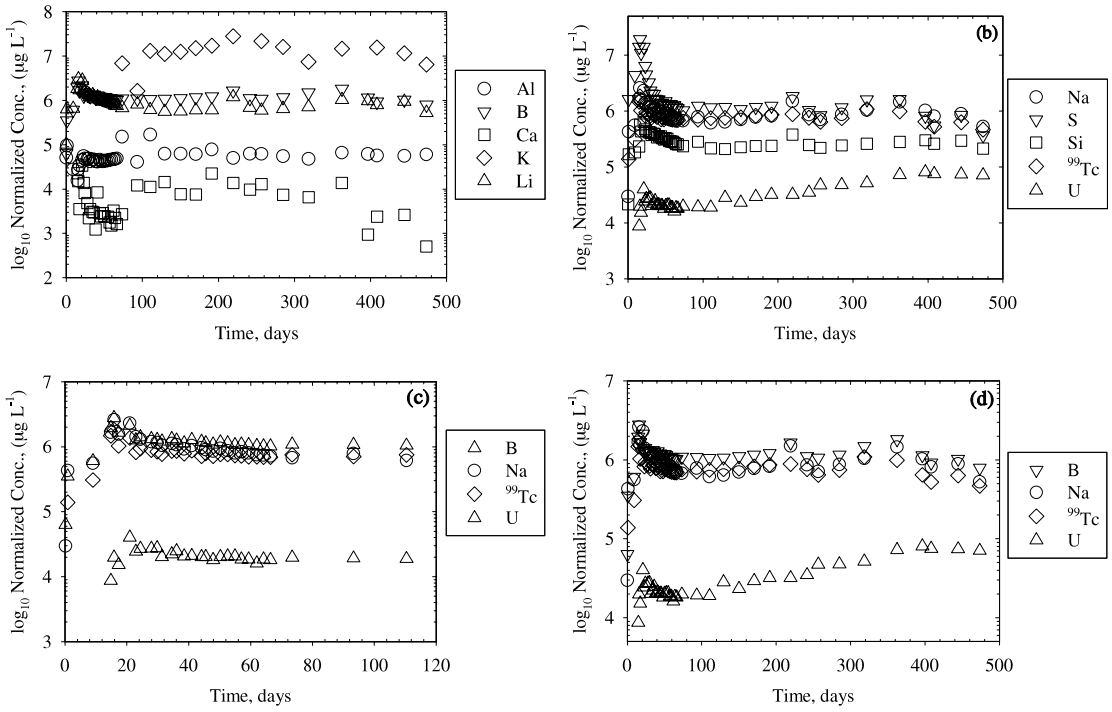

Fig. 4. Normalized concentration, in μg L^{-1}, for selected elements in the PUF test with LAWAN102 glass. The observed preferential release of K shown is not the result of the glass-water reaction, but the result of an underestimation of the K mass fraction for LAWAN102 glass.

where

c_i = effluent and background solution concentration of element i ($\mu g\ \ell^{-1}$)

f_i = mass fraction of element i in the glass (unitless).

The observed preferential release of *K* shown in Fig. 4 is not the result of the glass-water reaction, but the result of an underestimation of the *K* mass fraction for LAWAN102 glass. The results shown in Fig. 4 suggest that under these conditions B-, Li-, Na-, S-, and ^{99}Tc-bearing solid/mineral phase(s) are more soluble than Si-bearing solid/mineral phase(s) and much more soluble than Al-, Ca-, and U-bearing solid/mineral phase(s). Thermodynamic modeling of the effluent solutions with the EQ3NR geochemical code[42] (version 8.0) suggests the solutions may be supersaturated with respect to a number of alteration phases. The calculated saturation indices are supersaturated with respect to these phases because colloids smaller than the 0.2-μm average pore diameter of the porous plate are probably exiting the PUF column. Therefore, everything <0.2 μm was analyzed as being in solution. Transport within a PUF column is typically advection dominated. This can be demonstrated by calculating a Peclet (P_e) number for this experiment from Eq. (6):

$$P_e = \frac{\left(\frac{q}{\theta A}\right)x}{D} \ , \qquad P_e > 4 \text{ (advection-dominated system)} \ , \quad (6)$$

where

q = flow rate (2.31×10^{-11} m s^{-1})

θ = average volumetric water content (0.131 ± 0.003)

A = column area (2.85×10^{-4} m^2)

x = column distance (0.0762 m)

D = molecular diffusion coefficient for water (assumed to be 1.0×10^{-9} m^2 s^{-1}).

This calculation resulted in an average P_e number of 47. This value clearly shows that this PUF test is advection dominated. Similar results have been observed in PUF tests conducted with Pu-bearing waste forms in a can-in-canister configuration.[32,43]

III.C. Dissolution Rate

A comparison of the dissolution rates for the major components in LAWAN102 glass is shown in Figs. 5a and 5b. Similar to the concentration data, the rate of element release from the glass matrix decreases as the reaction time increases (Figs. 5a and 5b). This suggests that the value of the ion activity product is approaching equilibrium with respect to a rate-limiting alteration phase. Over the 1.5-yr test duration, the glass dissolution rate, based on B release, slowed from an initial rate of $\sim 0.10 \pm 0.03$ g m^{-2} day^{-1} to 0.010 ± 0.003 g m^{-2} day^{-1}. In comparison to previous PUF tests, the B release rate for LAWAN102 glass is approximately eight times lower than the Hanford LAW Product glass series[5] and within the experimental error of other ILAW glasses.[39] Therefore, these results indicate that LAWAN102 glass performs well and is a durable ILAW glass. As previously stated, B is considered the most reliable index for glass dissolution because it serves as a glass network former, like Si and Al, but is not sequestered by alteration phase(s) after being released from the glass.[37]

Glass dissolution rates based on ^{99}Tc and U, which are contaminants of concern, are shown in Fig. 5c and can be compared with the rate of matrix dissolution as indicated by B release. These results illustrate the release rate for B and ^{99}Tc are within the experimental error of one another, which suggests that ^{99}Tc is being released congruently from the glass. The incorporation of ^{99}Tc into alteration phases has been observed in static tests.[44,45] Mattigod et al.[44,45] observed that when ^{99}Tc-spiked Hanford Site groundwater was reacted with LAWABP1 glass at 160°C, ~5 to 12% of the ^{99}Tc was sequestered into reaction products (the secondary crystalline phases and hydrated gel layer that forms as a result of the glass-water reaction). Based on their results, Mattigod et al.[44,45] postulated that ^{99}Tc incorporation occurs mainly via isomorphic substitution in tetrahedral sites. Although ^{99}Tc incorporation into alteration phases has been observed in static tests, similar behavior was not observed under the dynamic, unsaturated flow conditions of the PUF test.

In contrast to ^{99}Tc, incongruent release is found for U, which has a release rate that is approximately 50 to 100 times lower than B and ^{99}Tc (see Fig. 5c). Geochemical modeling of the steady-state effluent analytical chemistry, with the EQ3NR code[42] (version 8.0), suggests that a uranyl phase (or phases) is controlling the transport of U, although U-containing alteration phases were not positively identified in posttest analyses of the reaction products. It is important to note that the geochemistry of uranium is complex. There are considerable differences or uncertainties in the stoichiometry and thermodynamic values assigned to uranium minerals, especially those exhibiting complex and variable compositions.[46] Therefore, solubility calculations based on the current knowledge of these values may have significant uncertainty and should be considered semiquantitative.

Although the majority of PUF tests to date have been conducted on nonradioactive glass samples, the results from LAWAN102 and LAWC22 allow a direct comparison between radioactive and nonradioactive ILAW glasses. This comparison is shown in Fig. 5c, where the dissolution rates, based on B, for LAWC22 and LAWAN102 are shown. The B steady-state rates for LAWC22 and LAWAN102 are within the experimental

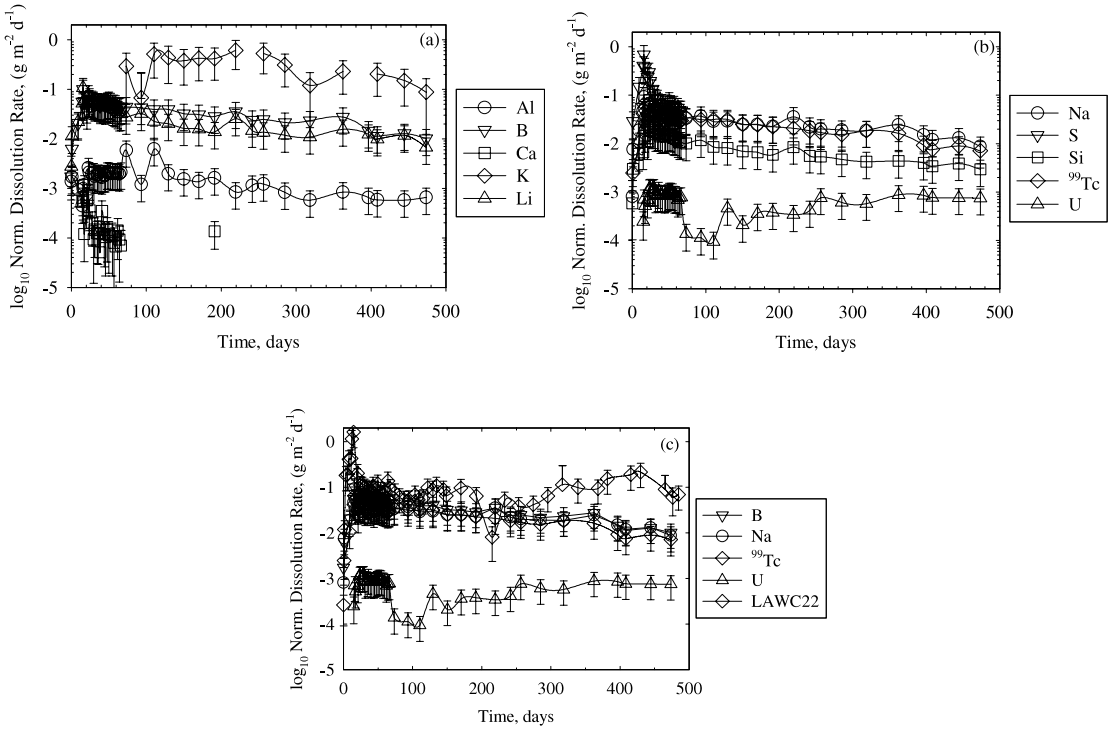

Fig. 5. Normalized dissolution rate in $g\,m^{-2}\,day^{-1}$ for selected elements released from the PUF test with LAWAN102 glass (a and b). A nonradioactive simulated glass, LAWC22, B release rate is shown for comparison in (c). The observed preferential release of K shown is not the result of the glass-water reaction but the result of an underestimation of the K mass fraction for LAWAN102 glass.

error of one another between the 10th and 300th day and suggest that a nonradioactive glass provided comparable results to a radioactive glass expected to be produced by the proposed WTP after 300 days of PUF testing. After day 300 the dissolution of LAWC22 becomes as much as ten times faster, $\sim 0.1\ g\,m^{-2}\,day^{-1}$, than LAWAN102. This may be the result of differences in the solubility controlling phase, which is discussed in Sec. III.D.

III.D. Analysis of Reaction Products

Figure 6 shows the posttest distribution of moisture in the PUF column as a function of depth. The data are unusual as compared with other ILAW glasses we have tested; the volumetric water content for each column section increases with depth away from the column inlet. In previous PUF tests with ILAW glasses, peaks in water content coincided with the onset of more extensive secondary phase formation (and consequent glass degradation), which is clearly not the case in this test. The observed decrease in the rate of water draining from the column around the 450th day suggests the 0.2-μm porous Ti plate was becoming plugged. The lack of drainage affected the uniform distribution of water within the column. Several attempts were made to reestablish this distribution, but they were unsuccessful and resulted in test termination. The lack of a uniform distribution of water within the column is evident by the posttest moisture content data points taken between 56 and 76 mm, which suggest the lower portion of the column is almost

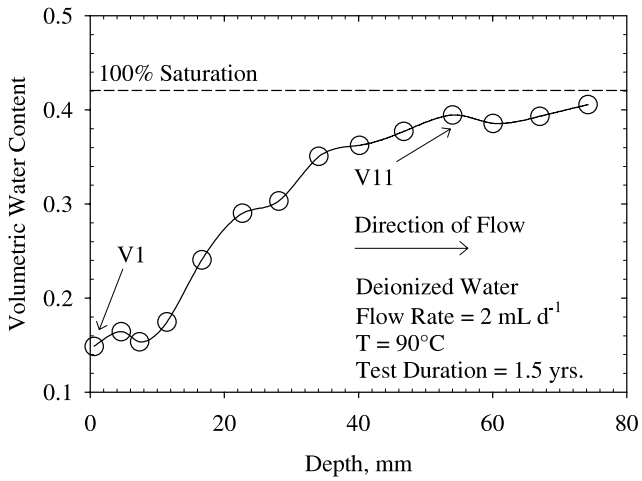

Fig. 6. Moisture fraction as a function of distance from the PUF column inlet for LAWAN102 glass. V1 and V11 refer to sample vials 1 and 11, respectively.

100% saturated (Fig. 6). As previously stated, other factors, such as changes in column porosity and hydraulic conductivity caused by changes in the hydraulic properties of the corroding glass, also have an effect on water content and were observed prior to day 450.

Scanning electron micrographs of unreacted and reacted grains are shown in Figs. 7 and 8. Analysis of the reacted grains revealed that sample V1 taken from the column inlet had the most extensive alteration observed (Fig. 7). As is typical of a PUF-reacted sample, glass alteration is observed only on portions of the grains that were in contact with water, whereas other areas remain pristine. A gel layer was observed on several reacted grains removed from the PUF test (Fig. 7b). Figures 7c and 7d show a reacted layer on the surface of glass particles with a claylike morphology, which has a composition, as determined by EDS, devoid of several glass components. The EDS analyses of this claylike phase (phase 1) indicate the presence of Al, Ca, Fe, Mg, O, Si, Ti, and Zn. In comparison to the pristine glass, phase 1 is enriched in Ca, Fe, Ti, and Zn; depleted in Cl, B, Na, Cl, and Zr; and contains relatively equal mass of Al and Si. A phase with similar morphology and chemistry was observed on grains removed from near the bottom of the column, sample V11. A magnification of grains from V1, Fig. 7c, indicates that phase 1 is growing out of the gel layer (see Fig. 7d); this suggests a corrosion sequence that starts with the glass-water interaction, progresses to the formation of a gel layer, and ends with the formation of phase 1 as the corroding glass approaches the final weathering state.

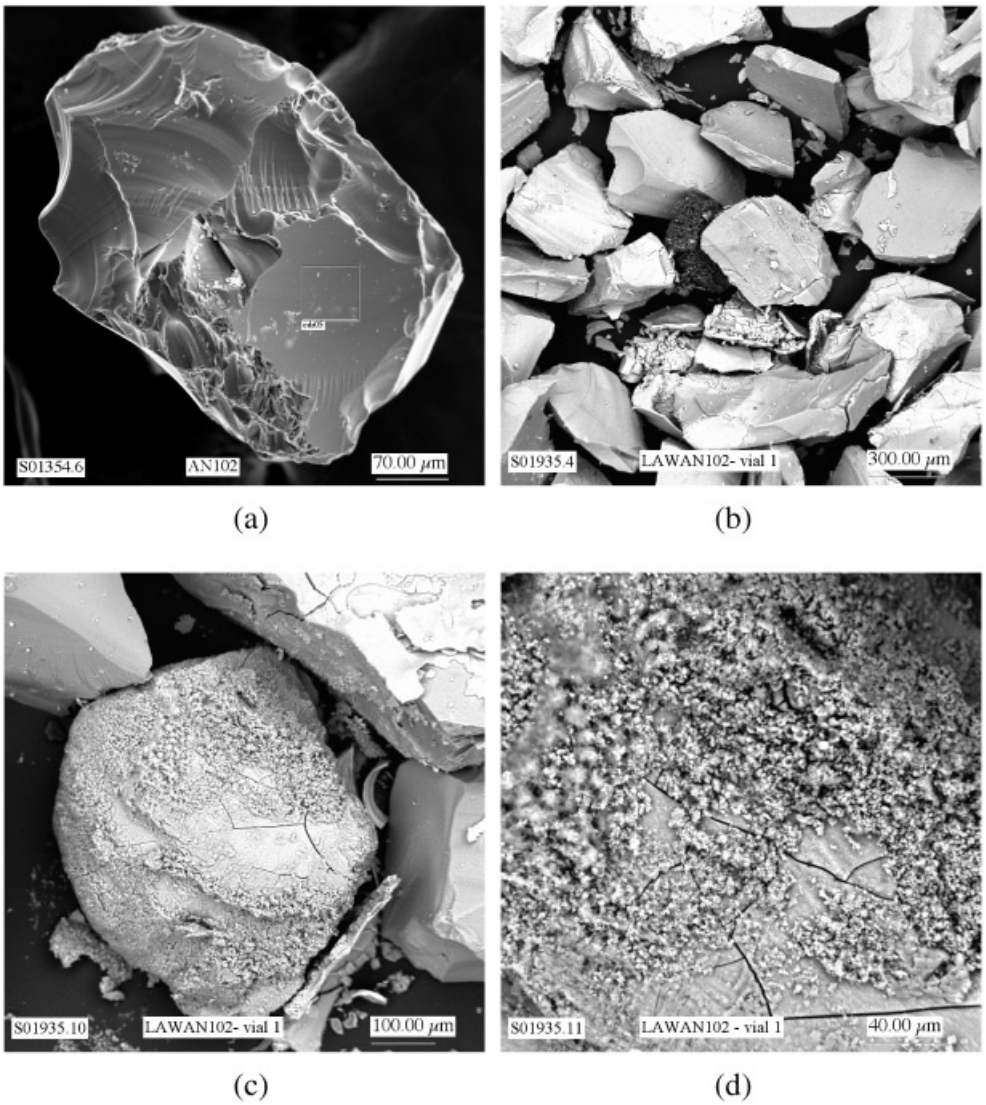

Fig. 7. SEM photographs of (a) an unreacted grain of LAWAN102 glass prior to testing and (b, c, and d) reacted grains of LAWAN102 glass after 560 days in a PUF test at flow rate = 2 mL day^{-1} and T = 90°C. The reacted grains were removed from the column inlet (referred to as V1 in Fig. 6).

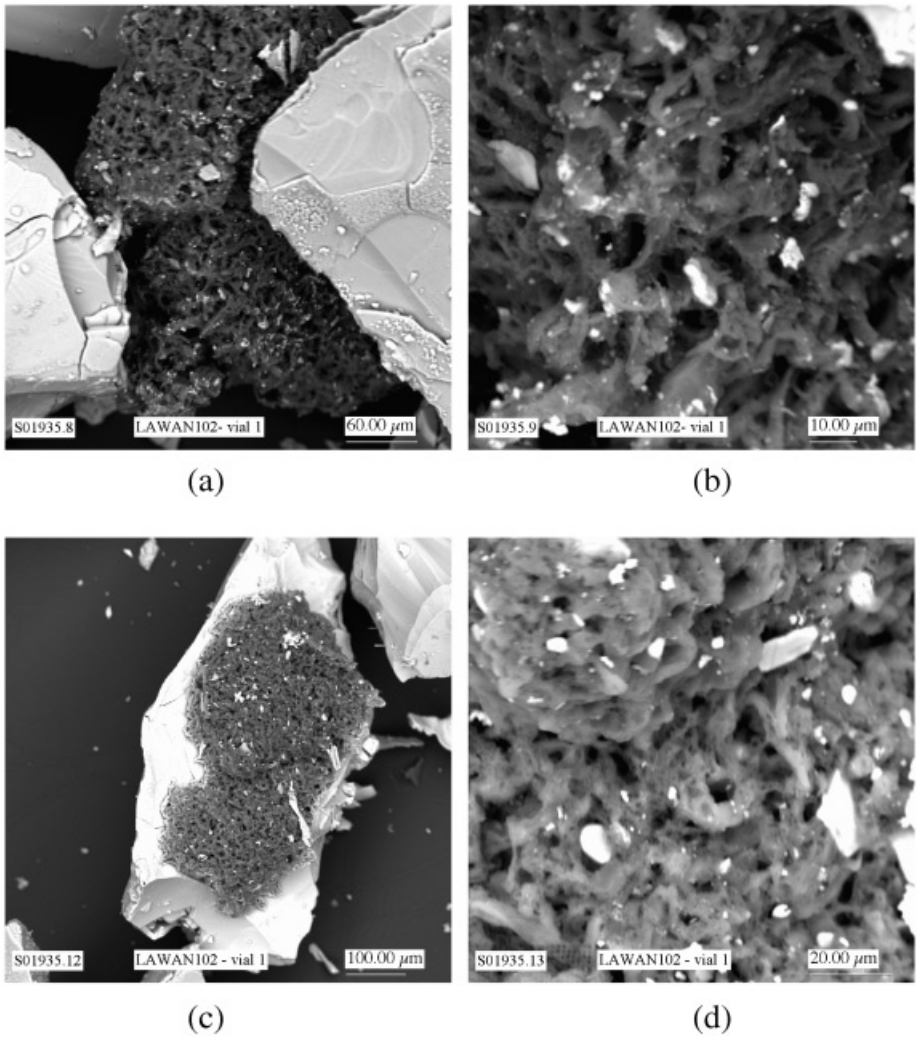

Fig. 8. SEM photographs of reacted grains of LAWAN102 glass after 560 days in a PUF test at $q = 2$ ml day^{-1} and $T = 90$°C. The photographs show evidence of another claylike phase (phase 2). The reacted grains were removed from the column inlet (referred to as V1 in Fig. 6). The lighter particles in (d) are enriched in Al and O, probably gibbsite (Al_2O_3), found on the surface of a reacted glass particle.

In addition to the gel layer and phase 1 that formed, another claylike phase (phase 2) with a different morphology and slightly different chemistry was also observed in sample V1 (see Fig. 8). The EDS analyses of phase 2 indicated the presence of Al, Ca, Cl, Fe, Mg, O, Si, and Zn. The material is enriched in Al, Fe, Mg, Si, and Zn, in comparison to the pristine glass. These results provide confirmation that Al and Si are being released from the glass and subsequently precipitating as alteration phases (i.e., phases 1 and 2) (see Fig. 5). Contrary to phase 1, phase 2 appears to be more developed and more porous, and it may form later in the paragenesis of the LAWAN102 glass corrosion process (Figs. 8a and 8b). The lighter particles shown in Figs. 8c and 8d are composed of Al and O, probably in the form of gibbsite (Al_2O_3), which was predicted by the use of the EQ3NR code[42] (version 8.0).

Bulk powder XRD was used in an attempt to identify both phases, phases 1 and 2, as well as any additional crystalline products. These analyses indicated that quartz was the only crystalline product present in a quantity >5 mass% in these samples. Transmission electron microscopy and XRD analysis of the unreacted glass after fabrication revealed a small amount of unreacted quartz,[36] which is added to the glass melt as a reagent. It is important to note that the formation of quartz is thermodynamically unfavorable under these test conditions; therefore, the quartz peak identified in the reacted samples via XRD was present in the starting material and is not a reaction product.

IV. RELEASE AND MOBILITY OF ^{99}Tc AND U FROM LAWAN102 GLASS

The release and transport of ^{99}Tc and U occur as the LAWAN102 glass-water reaction proceeds. When these elements are released from the corroding glass, the migration of ^{99}Tc and U occurs via different mechanistic processes because of their observed and known differences in chemical behavior. Technetium is released from the glass probably as the pertechnetate ion (TcO_4^-) under these oxidizing test conditions. Thermodynamic modeling of the steady-state effluent solution concentrations with the EQ3NR code[42] (version 8.0) suggested that 100% of the total dissolved ^{99}Tc is in the form of TcO_4^-. The anionic TcO_4^- complex is highly soluble and is not known to form significant aqueous complexes or discrete concentration-limiting solid phases under these test conditions. Static adsorption tests conducted with TcO_4^- illustrate that adsorption ranges from very low to zero under the alkaline pH conditions observed during this PUF test. Therefore, the lack of adsorption under these dynamic flow and transport conditions can be expected and provides a clearer explanation for the observed congruent release of ^{99}Tc from the PUF column.

As previously stated, the rate release of U suggests incongruent release from LAWAN102 glass that is probably the result of the formation of an alteration phase or phases. Contrary to ^{99}Tc, U can form several aqueous complexes under these test conditions. Thermodynamic modeling of the steady-state effluent solution concentrations with the EQ3NR code[42] (version 8.0) showed that 100% of the total dissolved U is distributed in the form of two aqueous uranyl-hydroxide species, $UO_2(OH)_3^-$ (70 to 75%) and $UO_2(OH)_2$ (aq) (25 to 30%). The presence of the $UO_2(OH)_3^-$ anionic complex, a poorly adsorbing U aqueous species, along with the one to two orders of magnitude difference between the U and B release rates make it highly unlikely that an adsorption process is the controlling transport mechanism. For additional details on the sorption of U, see Krupka et al.[47] and the references contained therein. Based on these results, we propose the transport of U is a kinetic mechanism that is probably being controlled by the formation and subsequent dissolution of a secondary phase(s). To explore this idea further, thermodynamic modeling with the EQ3NR code[42] (version 8.0) was conducted, and the results predicted the steady-state effluent solutions were saturated with respect to several possible uranyl-mineral and uranyl-solid phases. The thermodynamic stability of these possible phases was determined with the EQ3NR code[42] (version 8.0) by comparing the ion activity product (Q) to the equilibrium constant (K). The relationship between Q and K can be expressed mathematically by

$$SI = \log_{10}\left(\frac{Q}{K}\right) , \tag{7}$$

where SI is the saturation index (unitless). If $Q < K$ then $SI < 0$ and the solution is undersaturated, if $Q > K$ then $SI > 0$ and the solution is supersaturated, but if $Q = K$ then $SI = 0$ and the solution is in equilibrium (or near saturated) with respect to a potential solid phase.

A plot of SI as a function of time suggests that at least four uranyl-minerals and uranyl-solid phase(s) may be the solubility controlling phase or phases (Fig. 9). These include $CaUO_4$, clarkeite ($Na_2U_2O_7$), haiweeite

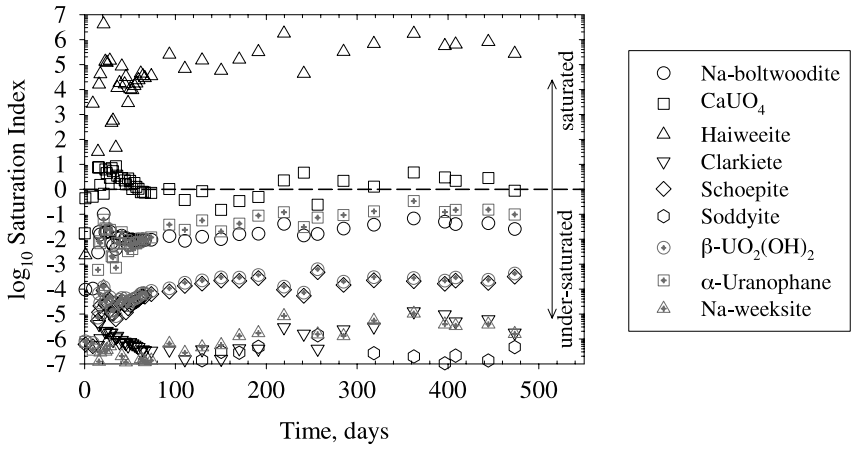

Fig. 9. The $\log_{10}$ saturation index (SI) as a function of time of possible uranyl-mineral and uranyl-solid phases based on thermodynamic modeling with the EQ3NR code[42] (version 8.0). Possible phase(s) include haiweeite [$Ca(UO_2)_2(Si_2O_5)_3 \cdot 5H_2O$], schoepite ($UO_3 \cdot xH_2O$), soddyite [$(UO_2)_2SiO_4 \cdot 2H_2O$], clarkeite ($Na_2U_2O_7$), and/or β-$UO_2(OH)_2$. Plotted are the uranyl phases with a $\log_{10}$SI > -8.0. Horizontal line provided as an eye guide to distinguish between uranyl phases that are undersaturated ($\log_{10} SI < 0$), nearly saturated ($\log_{10} SI = 0$), or oversaturated ($\log_{10} SI > 0$). The SI estimates given above for haiweeite were determined using the $\log_{10} K$ value at 25°C.

$[Ca(UO_2)_2(Si_2O_5)_3 \cdot 5H_2O]$, Na-boltwoodite ($NaUO_2SiO_3OH \cdot 1.5H_2O$), Na-weeksite $[Na_2(UO_2)_2Si_5O_{13} \cdot 3H_2O]$, schoepite ($UO_3 \cdot xH_2O$), soddyite $[(UO_2)_2SiO_4 \cdot 2H_2O]$, uranophane $[Ca(UO_2SiO_3OH)_2 \cdot 5H_2O]$, and β-$UO_2(OH)_2$. The $\log_{10} K$ values for the possible phases are listed in Table II. An enthalpy of formation estimate for the uranyl-mineral, haiweeite, was not available in the EQ3NR code (version 8.0) databases and is required to extrapolate the $\log_{10} K$ value from 25 to 90°C. The *SI* estimates given in Fig. 9 were determined from the $\log_{10} K$ value at 25°C and should be considered as an indication of the possibility for haiweeite formation based on the effluent solution chemistry. These results suggest one or all of these phases may be controlling the transport of U once it has been released from the corroding glass.

V. CONCLUSION

In contrast to other accelerated weathering test methods (UDT, VHT, and PCT), the PUF test method mimics the hydraulically unsaturated open-flow and transport conditions expected in the near-field environment, allows for the corroding waste form to achieve its final reaction state, and accelerates the hydrolysis and aging processes by as much as 50 times over conventional static tests. New experimental data on the alteration of a radioactive ILAW glass are provided and illustrate that rapid, sustained increases in the reaction-rate acceleration was not observed after 1.5 yr of PUF testing at 90°C and suggest that LAWAN102 glass is a durable ILAW glass. The PUF test with LAWAN102 glass also illustrates that the PUF technique monitors the complex coupling between (a) primary phase dissolution (e.g., ILAW glass), (b) alteration phase precipitation, and (c) unsaturated flow behavior, which includes changes in the hydraulic properties of the test material.

The transport of ^{99}Tc and U, two contaminants of concern, appears to occur via two separate mechanisms after each element is released from the glass. Congruent release of ^{99}Tc with B suggests that although incorporation of ^{99}Tc into alteration phases has been observed in static tests, similar behavior was not observed under the dynamic unsaturated flow conditions of the PUF test. The results from this experiment suggest that ^{99}Tc release will be controlled by the glass corrosion rate and secondary reactions will not inhibit ^{99}Tc migration into the vadose zone. Contrary to ^{99}Tc, the transport of U is being controlled by the glass corrosion rate and the formation of uranyl-minerals and/or uranyl-solid phases, probably $CaUO_4$, clarkeite ($Na_2U_2O_7$), haiweeite $[Ca(UO_2)_2(Si_2O_5)_3 \cdot 5H_2O]$, Na-Boltwoodite ($NaUO_2SiO_3OH \cdot 1.5H_2O$), Na-weeksite $[Na_2(UO_2)_2Si_5O_{13} \cdot 3H_2O]$, schoepite ($UO_3 \cdot xH_2O$), soddyite $[(UO_2)_2SiO_4 \cdot 2H_2O]$, uranophane $[Ca(UO_2SiO_3OH)_2 \cdot 5H_2O]$, and β-$UO_2(OH)_2$, although U-containing alteration phases were not positively identified in posttest analyses of the

TABLE II

$\log_{10} K$ Values for Select Uranyl-Mineral and Uranyl-Solid Phases

Formula	Reaction	$\log_{10} K$	Reference
$CaUO_4$	$CaUO_4 + 4H^+ \leftrightarrow Ca^{2+} + UO_2^{2+} + 2H_2O$	11.8576[a]	Grenthe et al.[48]
Clarkeite ($Na_2U_2O_7$)	$Na_2U_2O_7 + 6H^+ \leftrightarrow 2Na^2 + 2UO_2^{2+} + 3H_2O$	17.3471[a]	Grenthe et al.[48]
Haiweeite $[Ca(UO_2)_2(Si_2O_5)_3 \cdot 5H_2O]$	$Ca(UO_2)_2(Si_2O_5)_3 \cdot 5H_2O + 6H^+ \leftrightarrow Ca^{2+} + 2UO_2^{2+} + 6SiO_2(aq) + 8H_2O$	−7.0413[c]	Hemmingway[49]
Na-boltwoodite ($NaUO_2SiO_3OH \cdot 1.5H_2O$)	$NaUO_2SiO_3OH \cdot 1.5H_2O + 3H^+ \leftrightarrow Na^+ + UO_2^{2+} + SiO_2(aq) + 3.5H_2O$	4.5264[b]	Nguyen et al.,[50] Chen et al.[46]
Na-weeksite $[Na_2(UO_2)_2Si_5O_{13} \cdot 3H_2O]$	$Na_2(UO_2)_2Si_5O_{13} \cdot 3H_2O + 6H^+ \leftrightarrow 2Na^+ + 2UO_2^{2+} + 5SiO_2(aq) + 6H_2O$	3.0522[b]	Nguyen et al.,[50] Chen et al.[46]
Schoepite ($UO_3 \cdot xH_2O$)	$UO_3 \cdot 2H_2O + 2H^+ \leftrightarrow UO_2^{2+} + 3H_2O$	3.3340[a]	Grenthe et al.[48]
Soddyite $[(UO_2)_2SiO_4 \cdot 2H_2O]$	$(UO_2)_2SiO_4 \cdot 2H_2O + 4H^+ \leftrightarrow 2UO_2^{2+} + SiO_2(aq) + 4H_2O$	3.1197[b]	Chen et al.,[46] Moll et al.[51]
Uranophane $[Ca(UO_2SiO_3OH)_2 \cdot 5H_2O]$	$Ca(UO_2SiO_3OH)_2 \cdot 5H_2O \leftrightarrow Ca^{2+} + 2SiO_2(aq) + 2UO_2^{2+} + 9H_2O$	6.9037[b]	Chen et al.,[46] Perez et al.[52]
β-$UO_2(OH)_2$	$UO_2(OH)_2 + 2H^+ \leftrightarrow UO_2^{2+} + 2H_2O$	3.2089[a]	Grenthe et al.[48]

[a]Enthalpy of formation available to extrapolate $\log_{10} K$ value at 90°C

[b]EQ3NR uses pressure and temperature extrapolation to estimate the enthalpy of formation

[c]Enthalpy of formation value not available in database; $\log_{10} K$ could not be extrapolated to 90°C. Value provided is the $\log_{10} K$ at 25°C.

reaction products. This U-containing alteration phase will most likely form in the near-field disposal system environment and thereby limit the transport of U from the disposal system into the surrounding vadose zone. It is very difficult to translate the results from this laboratory experiment to what would be expected to happen in a disposal system environment. The results from other test methods, which evaluate different aspects of the glass-water interaction, the use of reactive transport simulators, and numerous other factors must be taken into consideration before using these results in performance assessment calculations. Some of these factors include but are not limited to (a) the chemistry of the Hanford Site pore water in contact with the ILAW glass, (b) the Hanford Site water infiltration rates, (c) the 15°C temperature of the disposal system, (d) the presence of canister metals, and (e) the engineered design for the disposal system. Therefore, only a few qualitative statements that discuss the performance of LAWAN102 glass and the release of ^{99}Tc and U from the glass have been made.

Finally, previous results and the results contained in this paper illustrate the need to understand the accelerated weathering of glasses and other waste forms with a test method that mimics the hydraulically unsaturated flow and transport conditions expected in a waste repository or disposal facility.

ACKNOWLEDGMENTS

The authors would like to acknowledge F. M. Mann at CH2M HILL Hanford Group, Inc. (Richland, Washington) for providing project funding and technical guidance. We would like to thank S. R. Baum and K. N. Geiszler, both of Pacific Northwest National Laboratory (PNNL), for completing the chemical analyses of the solution samples from our experiments. We are also grateful to R. M. Ermi of PNNL for conducting SEM and EDS analyses of the glass samples. The comments from two *Nuclear Technology* reviewers have assisted us in improving this manuscript. PNNL is operated for the U.S. Department of Energy by Battelle Memorial Institute.

REFERENCES

1. F. M. MANN, "Annual Summary of ILAW Performance Assessment for 2002," DOE/ORP-2000-19, Rev.1; CH2MHill Hanford Group, Inc. (2002).

2. Ecology; EPA; DOE Hanford Facility Agreement and Consent Order, As Amended, http://www.hanford.gov/tpa/tpahome.htm.

3. I. S. MULLER, A. C. BUECHELE, and I. L. PEGG, "Final Report: Glass Formulation and Testing with RPP-WTP-LAW Simulants," VSL-01R3560-2, Vitreous State Laboratory, Catholic University of America (2001).

4. J. D. VIENNA, "Preliminary ILAW Formulation Algorithm Description," 24590-LAW-RPT-RT-04-0003, Rev. 0; Bechtel National (2005).

5. B. P. McGRAIL, D. H. BACON, J. P. ICENHOWER, F. M. MANN, R. J. PUIGH, H. T. SCHAEF, and S. V. MATTIGOD, "Near-Field Performance Assessment for a Low-Activity Waste Glass Disposal System: Laboratory Testing to Modeling Results," *J. Nucl. Mater.*, **298**, 95 (2001).

6. B. P. McGRAIL and D. H. BACON, "Selection of a Computer Code for Hanford Low-Level Waste Engineered-System Performance Assessment," PNNL-10830, Rev. 1, Pacific Northwest National Laboratory (1998).

7. B. P. McGRAIL, D. H. BACON, R. J. SERNE, and E. M. PIERCE, "A Strategy to Assess Performance of Selected Low-Activity Waste Forms in an Integrated Disposal Facility," PNNL-14362, Pacific Northwest National Laboratory (2003).

8. B. P. McGRAIL, D. H. BACON, W. L. EBERT, and K. P. SARIPALLI, "A Strategy to Conduct an Analysis of the Long-Term Performance of Low-Activity Waste Glass in a Shallow Subsurface Disposal System at Hanford," PNNL-11834, Rev. 1, Pacific Northwest National Laboratory (2000).

9. J. K. BATES and T. J. GERDING, "One-Year Results of the NNWSI Unsaturated Test Procedure: SRL 165 Glass Application," ANL-85-41, Argonne National Laboratory (1986).

10. J. K. BATES, L. J. JARDINE, and M. J. STEINDLER, "Hydration Aging of Nuclear Waste Glass," *Science*, **218**, 51 (1982).

11. "Standard Test Methods for Determining Chemical Durability of Nuclear Waste Glasses: The Product Consistency Test (PCT)," ASTM C1285, pp. 1–10, American Society for Testing and Materials (1994).

12. C. M. JANTZEN and N. E. BIBLER, "Product Consistency Test (PCT) for DWPF Glass: Part 1, Test Development and Protocol," DPST-87-575, Savannah River Laboratory (1987).

13. J. K. BATES, J. W. EMERY, J. C. HOH, and T. R. JOHNSON, "Performance of High Plutonium-Containing Glasses for the Immobilization of Surplus Fissile Materials," in *Environmental Issues and Waste Management Technologies in the Ceramic and Nuclear Industries*, V. JAIN and R. PALMER, Eds., Vol. 61, pp. 447–454, American Ceramic Society, Westerville, Ohio (1995).

14. B. P. McGRAIL, J. P. ICENHOWER, P. F. MARTIN, H. T. SCHAEF, M. J. O'HARA, E. A. RODRIGUEZ, and J. L. STEELE, "Waste Form Release Data Package for the 2001 Immobilized Low-Activity Waste Performance Assessment," PNNL-13043, Rev. 2, Pacific Northwest National Laboratory (2001).

15. N. E. BIBLER, W. G. RAMSEY, T. F. MEAKER, and J. M. PAREIZS, "Durabilities and Microstructures of Radioactive Glasses for Immobilization of Excess Actinides at the Savannah River Site," *Proc. Material Research Symposium: Scientific Basis for Nuclear Waste Management XIX*, Pittsburgh,

Pennsylvania, November 27–December 1, 1995, Vol. 412, pp. 65–72, W. M. MURPHY and D. A. KNECHT, Eds., Materials Research Society (1996).

16. J. K. BATES, A. J. G. ELLISON, J. W. EMERY, and J. C. HOH, "Glass as a Waste Form for the Immobilization of Plutonium," *Proc. Materials Research Society Symposium: Scientific Basis for Nuclear Waste Management XIX*, Pittsburgh, Pennsylvania, November 27–December 1, 1995, pp. 57–64, W. M. MURPHY and D. A. KNECHT, Eds., Materials Research Society (1996).

17. W. L. EBERT and J. K. BATES, "A Comparison of Glass Reaction at High and Low Glass Surface/Solution Volume," *Radioact. Waste Manage.*, **104**, 372 (1993).

18. W. L. EBERT and S.-W. TAM, In "Dissolution Rates of DWPF Glasses from Long-Term PCT," *Materials Research Society Symposium: Scientific Basis for Nuclear Waste Management XX*, Pittsburgh, Pennsylvania, December 2–6, 1996, W. J. GRAY and I. R. TRIAY, Eds., pp. 149–156, Materials Research Society (1997).

19. W. G. RAMSEY, N. E. BIBLER, and T. F. MEAKER, "Compositions and Durabilities of Glasses for Immobilization of Plutonium and Uranium," *Waste Management*, Tucson, Arizona, February 26–March 2, 1995, pp. 23828–23907, Waste Management Symposia, Inc. (1995).

20. J. W. SHADE, and D. M. STRACHAN, "Effect of High Surface Area to Solution Volume Ratios on Waste Glass Leaching," *Ceramic Aware! Bull.*, **65**, *12*, 1568 (1986).

21. "High-Level Borosilicate Waste Glass: A Compendium of Corrosion Characteristics, Vol. 1," DOE-EM-0177, U.S. Department of Energy Office of Waste Management (1994).

22. "High-Level Waste Borosilicate Glass: A Compendium of Corrosion Characteristics, Vol. 2," DOE-EM-0177, U.S. Department of Energy Office of Waste Management (1994).

23. A. JIRICKA, J. D. VIENNA, P. R. HRMA, and D. M. STRACHAN, "The Effect of Experimental Conditions and Evaluation Techniques on the Alteration of Low Activity Glasses by Vapor Hydration," *J. Non-Crystal. Solids*, **292**, *1–3*, 25 (2001).

24. B. P. McGRAIL, P. F. MARTIN, C. W. LINDENMEIER, and H. T. SCHAEF, "Application of the Pressurized Unsaturated Flow (PUF) Test for Accelerated Ageing of Waste Forms," *Proc. Int. Conf. Ageing Studies and Lifetime Extension of Materials*, Oxford, United Kingdom, July 12–14, 1999.

25. C. L. CRAWFORD, D. M. FERRARA, R. F. SCHUMACHER, and N. E. BIBLER, "Crucible-Scale Active Vitrification Testing Envelope C, Tank 241-AN-102 (U)," WSRC-TR-2000-00371, SRT-RPP-2000-00022, Rev. 0, formerly BNF-003-98-0271, Westinghouse Savannah River Company (2001).

26. C. NASH, "Strontium-Transuranic Precipitation and Crossflow Filtration of 241-AN-102 Large C," WSRC-TR-2000-00506, SRT-RPP-2001-00006, formerly BNF-03-98-0317, Westinghouse Savannah River Company (2000).

27. W. D. KING, N. M. HASSAN, and D. J. McCABE, "Intermediate-Scale Ion Exchange Removal of Cesium and Technetium from Hanford Tank 241-AN-102," WSRC-TR-2000-00420, SRT-RPP-2000-00024, Westinghouse Savannah River Company (2000).

28. "Standard Test Methods for Sieve Analysis of Fine and Coarse Aggregates," ASTM C136, pp. 1–10, American Society for Testing and Materials (2001).

29. B. P. McGRAIL, W. L. EBERT, A. J. BAKEL, and D. K. PEELER, "Measurement of Kinetic Rate Law Parameters on a Na-Ca-Al Borosilicate Glass for Low-Activity Waste," *J. Nucl. Mater.*, **249**, 175 (1997).

30. B. P. McGRAIL, J. P. ICENHOWER, P. F. MARTIN, D. R. RECTOR, H. T. SCHAEF, E. A. RODRIGUEZ, and J. L. STEELE, "Low-Activity Waste Glass Studies: FY2000 Summary Report," PNNL-13381, Pacific Northwest National Laboratory (2000).

31. D. WOLFF-BOENISCH, S. R. GISLASON, E. H. OELKERS, and C. PUTNIS, "The Dissolution Rates of Natural Glasses as a Function of Their Composition at pH 4 and 10.6, and Temperatures from 25 to 74°C," *Geochim. Cosmochim. Acta*, **68**, *23*, 4843 (2004).

32. B. P. McGRAIL, P. F. MARTIN, H. T. SCHAEF, C. W. LINDENMEIER, and A. T. OWEN, "Glass/Ceramic Interactions in the Can-In-Canister Configuration for Disposal of Excess Weapons Plutonium," *Proc. Material Research Symposium: Scientific Basis for Nuclear Waste Management XXIII*, Boston, Massachusetts, November 29–December 2, 1999, pp. 345–352, R. W. SMITH and D. W. SHOESMITH, Eds., Material Research Society (2000).

33. B. P. McGRAIL, C. W. LINDENMEIER, P. F. MARTIN, and G. W. GEE, "The Pressurized Unsaturated Flow (PUF) Test: A New Method for Engineered-Barrier Materials Evaluation," in *Environmental Issues and Waste Management Technologies in the Ceramic and Nuclear Industries II*, V. JAIN and D. K. PEELER, Eds., Vol. 72, pp. 317–329, The American Ceramic Society, Westerville, Ohio (1996).

34. B. P. McGRAIL, C. W. LINDENMEIER, and P. F. MARTIN, "Characterization of Pore Structure and Hydraulic Property Alteration in Pressurized Unsaturated Flow Tests," *Proc. Material Research Symposium: Scientific Basis for Nuclear Waste Management*, Warrendale, Pennsylvania, November 30–December 4, 1998, pp. 421–428, D. J. WRONKIEWICZ and J. H. LEE, Eds., Materials Research Society (1999).

35. P. J. WIERENGA, M. H. YOUNG, G. W. GEE, R. G. HILLS, C. T. KINCAID, T. J. NICHOLSON, and R. E. CADY, "Soil Characterization Methods for Unsaturated Low-Level Waste Sites," PNL-8480, Pacific Northwest Laboratory (1993).

36. B. P. McGRAIL, J. P. ICENHOWER, D. H. BACON, J. D. VIENNA, K. P. SARIPALLI, H. T. SCHAEF, P. F. MARTIN, R. D. ORR, E. A. RODRIGUEZ, and J. L. STEELE, "Low-Activity Waste Glass Studies: FY2002 Summary Report," PNNL-14145, Pacific Northwest National Laboratory (2002).

37. B. E. SCHEETZ, W. P. FREEBORN, D. K. SMITH, C. ANDERSON, and M. ZOLENSKY, "The Role of Boron in Monitoring the Leaching of Borosilicate Glass Waste Forms," *Proc. Material Research Society Symposium*, Boston, Massachusetts, November 26–29, 1984, pp. 129–134, Materials Research Society (1985).

38. B. P. McGRAIL, P. F. MARTIN, and C. W. LINDENMEIER, "Accelerated Testing of Waste Forms Using a Novel Pressurized Unsaturated Flow Method," *Proc. Materials Research Society Symposium: Scientific Basis for Nuclear Waste Management XX*, Pittsburgh, Pennsylvania, 1997, pp. 253–260, W. J. GRAY and I. R. TRIAY, Eds., Materials Research Society (1997).

39. E. M. PIERCE, B. P. McGRAIL, E. A. RODRIGUEZ, H. T. SCHAEF, K. P. SARIPALLI, R. J. SERNE, K. M. KRUPKA, P. F. MARTIN, S. R. BAUM, K. N. GEISZLER, L. R. REED, and W. J. SHAW, "Waste Form Release Data Package for the 2005 Integrated Disposal Facility Performance Assessment," PNNL-14805, Pacific Northwest National Laboratory (2004).

40. J. L. CONCA and J. WRIGHT, "Hydrostratigraphy and Recharge Distribution from Direct Measurements of Hydraulic Conductivity Using the UFA Method," PNL-9424, Pacific Northwest National Laboratory (1992).

41. A. P. GAMERDINGER and D. I. KAPLAN, "Application of a Continuous-Flow Centrifugation Method for Solute Transport in Disturbed, Unsaturated Sediments and Illustration of Mobile-Immobile Water," *Water Resour. Res.*, **36**, *7*, 1747 (2000).

42. T. J. WOLERY, "EQ3NR, A Computer Program for Geochemical Aqueous Speciation-Solubility Calculations: Theoretical Manual, User's Guide, and Related Documentation (Version 7.0)," UCRL-MA-110662 PT III, pp. 1–246, Lawrence Livermore National Laboratory (1992).

43. E. M. PIERCE, B. P. McGRAIL, J. MARRA, P. F. MARTIN, B. W. AREY, and K. N. GEISZLER, "Accelerated Weathering of a High-Level and Pu-Bearing Lanthanide Borosilicate Waste Glass in a Can-In-Canister Configuration," *Appl. Geochem.* (accepted for publication).

44. S. V. MATTIGOD, R. J. SERNE, B. P. McGRAIL, and V. L. LEGORE. In "Radionuclide Incorporation in Secondary Crystalline Minerals from Chemical Weathering of Waste Glasses," *Materials Research Society Symposium*, Warrendale, Pennsylvania, November 26–29, 2001, pp. 597–606, Materials Research Society (2002).

45. S. V. MATTIGOD, R. J. SERNE, V. L. LEGORE, K. E. PARKER, R. D. ORR, D. E. McCREADY, and J. S. YOUNG, "Radionuclide Incorporation in Secondary Crystalline Minerals Resulting from Chemical Weathering of Selected Waste Glasses: Progress Report: Task kd.5b," PNNL-14391, Pacific Northwest National Laboratory (2003).

46. F. CHEN, R. C. EWING, and S. B. CLARK, "The Gibbs Free Energies and Enthalpies of Formation of U^{6+} Phases: An Empirical Method of Prediction," *Am. Mineral.*, **84**, 650 (1999).

47. K. M. KRUPKA, D. I. KAPLAN, S. V. MATTIGOD, and R. J. SERNE, "Understanding Variation in Partition Coefficient, K_d, Values: Volume II. Review of Geochemistry and Available K_d Values for Cadmium, Cesium, Chromium, Lead, Plutonium, Radon, Strontium, Thorium, Tritium (^3H), and Uranium," EPA-402-R-99-004B, Environmental Protection Agency (1999).

48. I. GRENTHE, J. FUGER, R. J. M. KONINGS, R. J. LEMIRE, A. B. MULLER, C. NGUYEN-TRUNG, and H. WANNER, *Chemical Thermodynamics of Uranium*, North-Holland/Elsevier, New York (1992).

49. B. S. HEMINGWAY, "Thermodynamic Properties of Selected Uranium Compounds and Aqueous Species at 298.15 K and 1 bar and at Higher Temperatures—Preliminary Models for the Origin of Coffinite Deposits," Open-File Report 82-619; pp. 1–90, U.S. Geological Survey (1982).

50. S. N. NGUYEN, R. J. SILVA, H. C. WEED, and J. E. J. ANDREWS, "Standard Gibbs Free Energies of Formation at the Temperature 303.15K of Four Uranyl Silicates: Soddyite, Uranophane, Sodium Boltwoodite, and Sodium Weeksite," *J. Chem. Thermodyn.*, **24**, 359 (1992).

51. H. MOLL, G. GEIPEL, W. MATZ, G. BERNARD, and H. NITSCHE, "Solubility and Speciation of $(UO_2)_2SiO_4 \cdot 2H_2O$ in Aqueous Systems," *Radiochim. Acta*, **74**, 3 (1996).

52. I. PEREZ, I. CASAS, M. MARTIN, and J. BRUNO, "The Thermodynamics and Kinetics of Uranophane Dissolution in Bicarbonate Test Solutions," *Geochim. Cosmochim. Acta*, **64**, *4*, 603 (2000).